

Microstructure and Magnetic Properties of Fe-Cr-Co Alloys

著者	岡田 益男
journal or publication title	IEEE Transactions on Magnetics
volume	14
number	4
page range	245-252
year	1978
URL	http://hdl.handle.net/10097/46457

- [9] J. H. P. Watson, "Theory of capture of particles in magnetic high-intensity filters," *IEEE Trans. Magn.* MAG-11, 1579-99, (1975).
- [10] C. Cowan, F. J. Friedlaender, R. Jaluria, "Single wire model of high gradient magnetic separation processes II," *IEEE Trans. Magn.*, MAG-12, 466-60 (1976).
- [11] Z. J. J. Stekly and J. V. Minervini, "Shape effect of the matrix on the capture cross-section of particles in a high gradient magnetic separator," *IEEE Trans. Magn.* MAG-12, 474-9 (1976).
- [12] D. L. Cummings, D. C. Prieve and G. J. Powers, "The motion of small paramagnetic particles in a high gradient magnetic separator," *IEEE Trans. Magn.* MAG-12, 471-3 (1976).
- [13] H. K. Collan, M. Kokkala, A. Ritvos, Viejo Pohjola and Vieko Pohjola, "Rapid Evaluation of magnetic filter performance," *IEEE Trans. Magn.*, MAG-13, 1480-2, (1977).
- [14] I. Y. Akoto, "Mathematical modelling of high-gradient magnetic separation devices," *IEEE Trans. Magn.* MAG-13, 1486-9, (1977).
- [15] J. Iannicelli, "High extraction magnetic filtration of Kaolin Clay and mineral slimes," *Filtration and Separation* Jan/Feb (1976) pp. 15-17.
- [16] C. J. Lin, Y. A. Liu, D. L. Vives, M. J. Oak, G. E. Crow and E. L. Huffman, "Pilot-scale studies of sulfur and ash removal from coals by high gradient magnetic separation," *IEEE Trans. Mag.* MAG-12, 513-521 (1976).
- [17] R. R. Oder, "High gradient magnetic separation theory and applications," *IEEE Trans. Magn.* MAG-12, 428-435 (1976).
- [18] P. W. Riley and J. H. P. Watson, "The use of paramagnetic matrices for magnetic separations," *Filtration and Separation* July/Aug (1977).
- [19] R. R. Oder and C. R. Price, "HGMS: Mathematical modelling of commercial practice," *AIP Conference Proc. No. 29* 641-643 American Inst. of Phys. (1975).
- [20] J. H. P. Watson and D. Hocking, "The beneficiation of clay using a superconducting magnetic separator," *IEEE Trans. Magn.* MAG-11, (1975).

Microstructure and Magnetic Properties of Fe-Cr-Co Alloys

MASUO OKADA, GARETH THOMAS, MOTOFUMI HOMMA, AND HIDEO KANEKO, MEMBER, IEEE

Abstract—The microstructures of an Fe-31wt%Cr-23wt%Co ductile permanent magnet alloy after isothermal aging, thermomagnetic treatment, and step aging have been characterized by transmission electron microscopy and by measurement of the Curie temperature. Isothermal aging itself produces the undesirable microstructure. Aging at 600°C develops the magnetic chromium-rich phase. Aging at 600°C produces a nonmagnetic chromium-rich phase dispersed within the iron-rich phase. The effect of thermomagnetic treatment on the microstructure of the alloy is discussed in comparison with that of Alnico alloys. Step aging produces the desirable microstructure, viz., the elongated ferromagnetic phase imbedded in the paramagnetic phase.

INTRODUCTION

IT IS KNOWN that Fe-Cr-Co alloys are potentially ductile hard magnets. These alloys were designed by following the miscibility gap in the Fe-Cr system into the Fe-Cr-Co ternary system [1]. The shape of the miscibility gap in the Fe-Cr-Co system is now well established [2].

Manuscript received October 27, 1977; revised February 8, 1978. This work was supported by the U.S. Department of Energy through Lawrence Berkeley Laboratory, University of California, Berkeley, CA 94720.

M. Okada and G. Thomas are with the Department of Materials Science and Engineering, College of Engineering, University of California, Berkeley, and the Materials and Molecular Research Division, Lawrence Berkeley Laboratory, University of California, Berkeley.

M. Homma and H. Kaneko are with the Department of Materials Science, Faculty of Engineering, Tohoku University, Sendai, Japan 980.

The magnetic hardening of the alloys is associated with decomposition within the miscibility gap producing modulated structures, consisting of two phases, an iron-rich phase (α_1) and a chromium-rich phase (α_2). The features of the decomposition are consistent with those expected from spinodal decomposition of the high-temperature phase (α) during aging [1], [3].

In order to control the magnetic properties of materials, it is important to characterize and control their microstructures. However, no systematic studies of the microstructure of these alloys have been reported. Thus the purpose of the present investigation is to establish some of the microstructure-property relationships in Fe-Cr-Co alloys resulting from a series of heat treatments (isothermal aging, thermomagnetic treatment, and step aging). Since the microstructural changes occur on such a fine scale, transmission electron microscopy must be employed for characterization [4].

EXPERIMENTAL PROCEDURES

An Fe-31wt%Cr-23wt%Co alloy was chosen for the present investigation because the decomposition tie line of the alloy is well established [2].

The alloy was melted in an induction furnace from 99.9% electrolytic iron, 99.9% electrolytic chromium, and 99.9% cobalt. Chemical analysis verified that the final alloy was

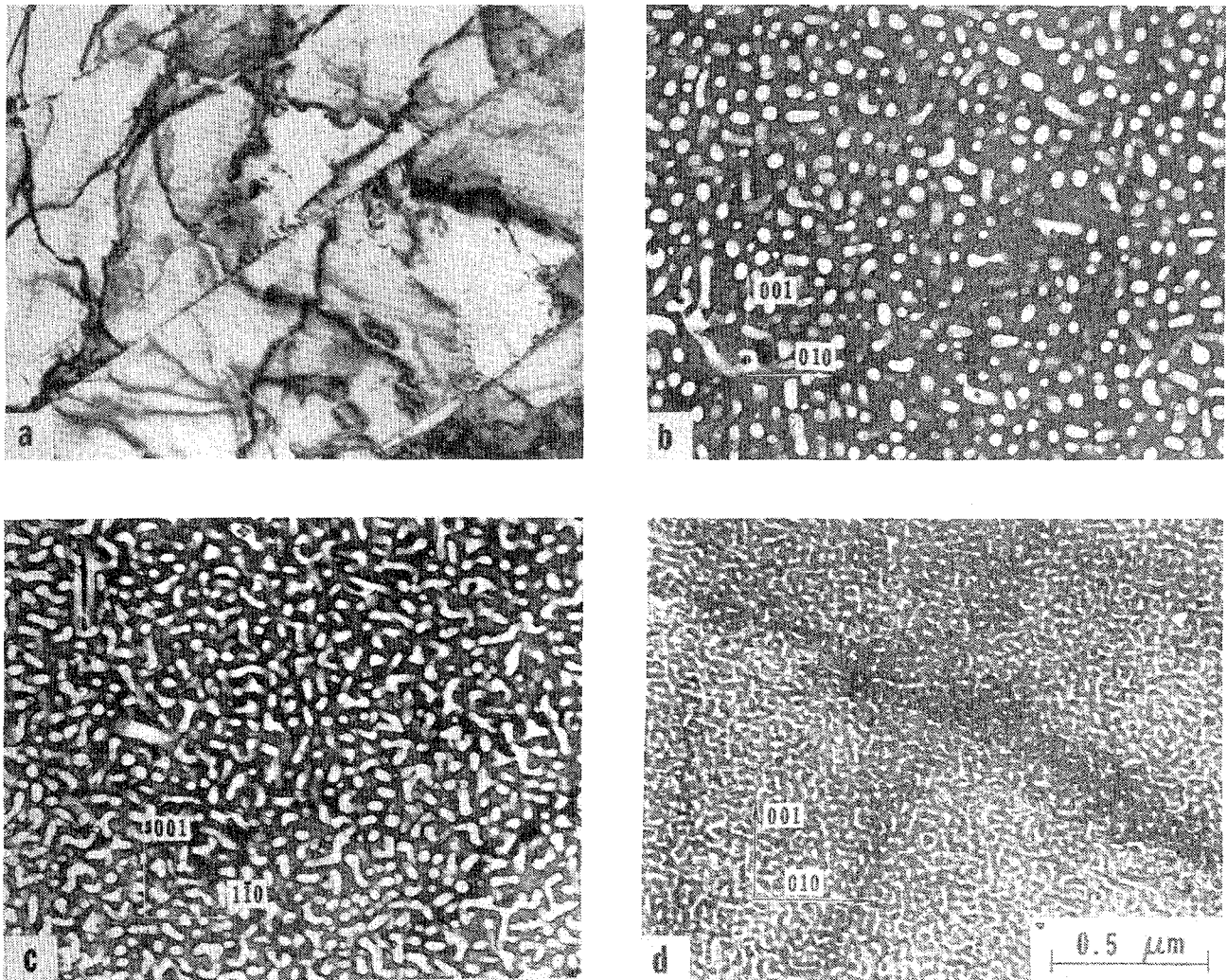


Fig. 1. Bright field micrographs of Fe-31wt%Cr-23wt%Co alloy aged for 1 h. (a) At 680°C. (b) At 670°C. (c) At 660°C (d) At 650°C.

within 1% of the desired composition. The ingot was then placed in a quartz tube, homogenized for one day at 1300°C and quenched in water. Slices, 0.5-mm thick, were cut and solution treated at 1300°C for 30 min under argon atmosphere in a vertical resistance furnace. Specimens were then quenched from 1300°C in iced brine at a rate of over 100°C/s to avoid γ or σ phase formation.

The changes in microstructure, volume fraction of phases, and wavelength (interrod spacing) were established by electron microscopy and diffraction, including high-resolution lattice imaging [4] and the utilization of laser optical diffraction [5], [6]. Electron microscopy disc specimens were thinned in an automatic jet polisher using an electrolytic solution of 23% perchloric acid and 77% acetic acid. The composition fluctuations were deduced by measuring the Curie temperature of the decomposed Cr-rich phase (α_2) [7]. Since the Curie temperature of the α_1 phase is approximately 900°C [8], measurements well below 900°C can be directly related to the composition of the α_2 phase. The magnetization as a function of temperature was measured with a magnetic balance while the specimen was heated at a rate of 10°C/min.

RESULTS

A. Isothermal Aging

The series of bright field micrographs shown in Fig. 1 were taken from the alloy aged for 1 h at 680°C, 670°C, 660°C, and 650°C, respectively. The phase with bright contrast is identified as the α_1 phase, the phase with dark contrast as the α_2 phase. These micrographs reveal that the miscibility gap of the alloy is below 670°C and also show that the morphology of the aged microstructure is very sensitive to the aging temperature. At the lower aging temperatures the dispersion is finer and the two phases more interconnected with rod-like shapes.

The microstructures shown in Fig. 2 were obtained from the alloy aged at 640°C for 3 min, 20 min, 2 h, and 20 h. The decomposition process appears to be isotropic in the alloy and is associated with halo-type diffuse satellites in the corresponding diffraction pattern, as shown in Fig. 3. The radius of these diffuse satellites decreases with aging time as the modulation wavelength increases. This behavior is typical of spinodal coarsening [7]. After prolonged aging the α_1 phase becomes

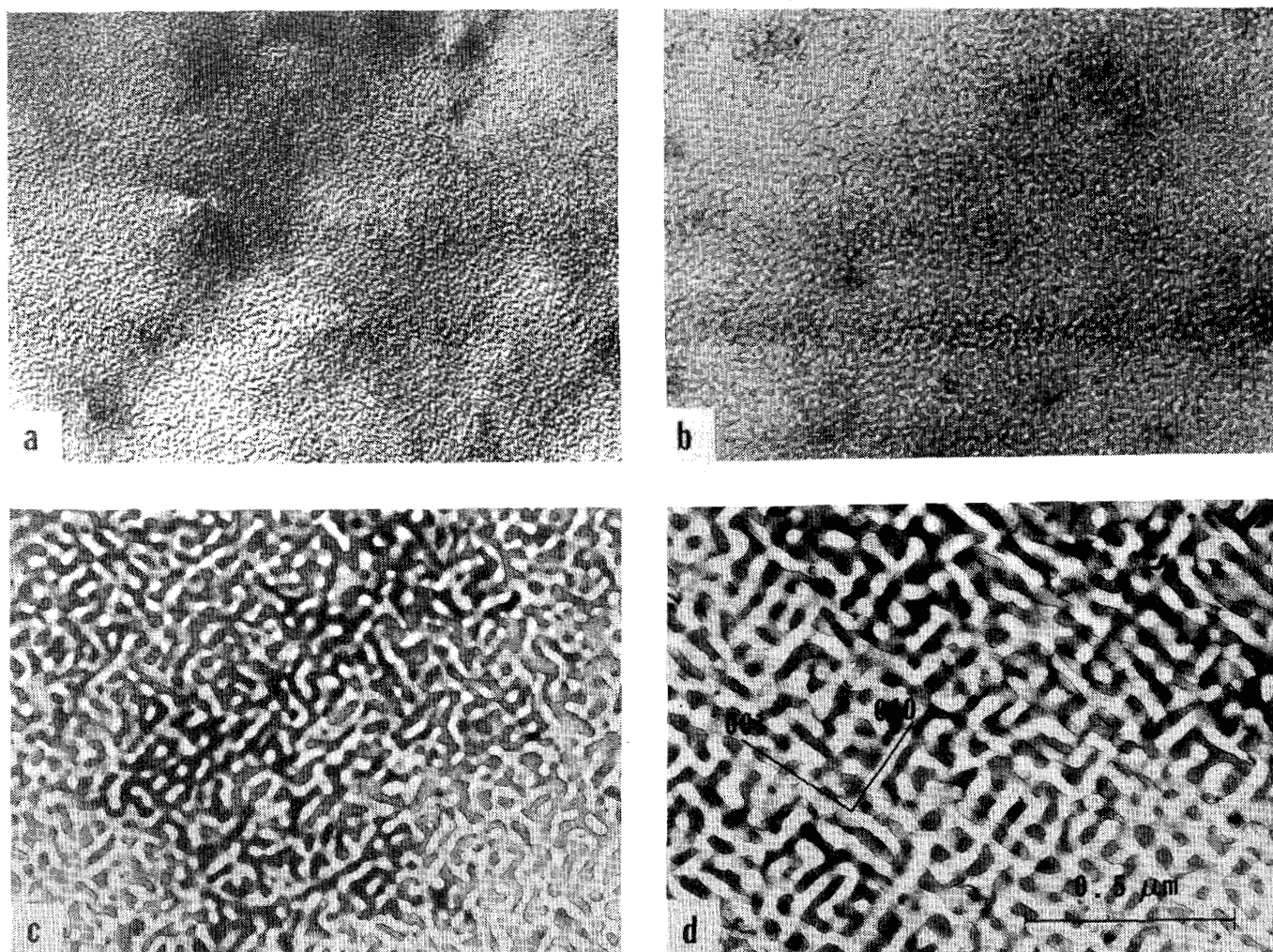


Fig. 2. Bright field micrographs of alloy at 640°C. (a) For 3 min. (b) For 20 min, $H_c \sim 100$ Oe. (c) For 2 h, $H_c \sim 160$ Oe. (d) For 20 h, $H_c \sim 125$ Oe.

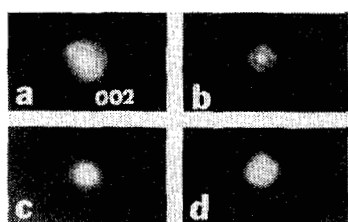


Fig. 3. Satellites around (002) reflections in corresponding diffraction patterns of Fig. 1.

aligned along the $\langle 100 \rangle$ directions, as shown in Fig. 2(c), (d), and this produces peaking along $\langle 100 \rangle$ in the diffraction pattern of Fig. 3(c), (d).

The micrographs shown in Fig. 4 are taken from the alloy aged at 600°C for 20 min, 2 h, 100 h, and 500 h. The main difference in microstructures between Fig. 2 and Fig. 4 is that the α_2 phase is the major phase in Fig. 2 and the minor one in Fig. 4. This can be understood from the asymmetry in shape of the miscibility gap in the Fe-Cr-Co system [2]. As the aging temperature is changed, different tie lines are encountered, and the volume fractions of α_1 and α_2 phases

change. In the present alloy equal fractions of the two phases would be obtained by aging near 635°C. Thus small changes in aging temperature can produce large changes in microstructural distributions of the α_1 and α_2 phases.

Figure 5(a) shows a high-resolution (110) lattice image taken from the alloy aged at 660°C for 1 hr (see Fig. 1(c)). The (110) fringes appear to be continuous across the interface between the α_1 and α_2 phases. The difference in lattice parameters of the two phases was detected by laser optical diffraction as shown in Fig. 5(b) [5]. This experiment provides direct evidence that both phases are coherent.

The magnetization as a function of temperature for the alloy aged at 640°C is illustrated in Fig. 6. The magnetization of the specimens in the "as quenched" and aged states decreases with temperature up to approximately 400°C and then increases above 400°C and has a small peak. The magnetization curve is found to be reversible up to 400°C, but irreversible above 400°C, suggesting that the composition of the two phases does not change during heating up to 400°C.

In Fig. 6 the magnetization curve of specimen *B* aged at 640°C for 20 min changes slope around 310°C, which is identi-

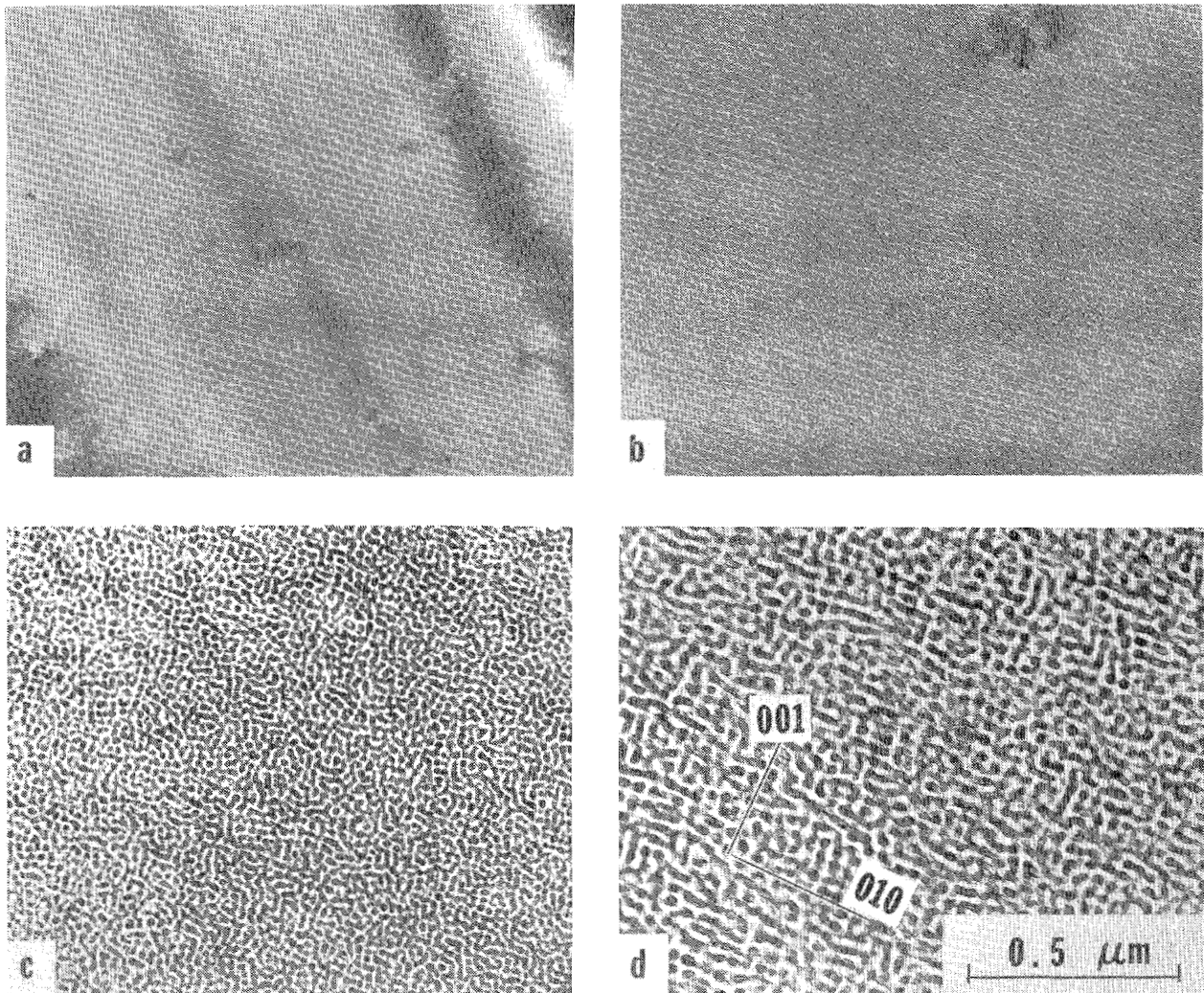


Fig. 4. Micrographs of alloy aged at 600°C. (a) For 20 min, $H_c \sim 15$ Oe. (b) For 2 h, $H_c \sim 35$ Oe. (c) For 100 h, $H_c \sim 200$ Oe. (d) For 500 h, $H_c \sim 260$ Oe.

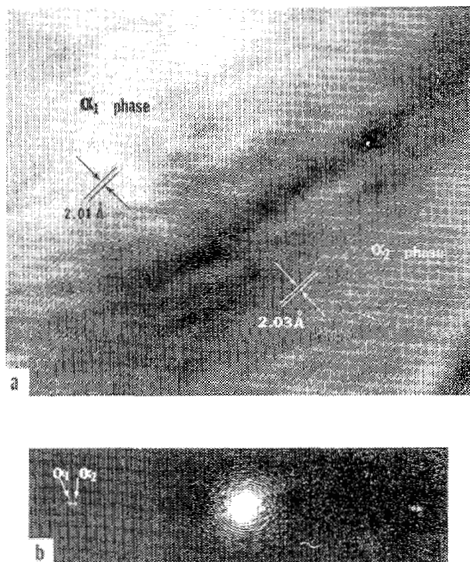


Fig. 5. (a) High-resolution (110) lattice image of alloy aged at 660°C for 1 h. (b) Corresponding laser optical diffraction pattern.

fied as the Curie temperature of the α_2 phase [2]. The longer the aging time, the sharper the discontinuity in the slope of this curve appears. The Curie temperature of the α_2 phase aged at various temperatures as a function of aging time is summarized in Fig. 7. These results suggest: 1) that the decomposed phases reach their equilibrium composition within almost two hours; 2) that the α_2 phase developed during aging at 600°C is nonmagnetic at room temperature, but is magnetic after aging at 640°C or 620°C. These results illustrate the sensitivity of the properties to aging temperature, which means precipitate composition and morphology.

B. Thermomagnetic Treatment

Thermomagnetic treatments play an important role in producing good magnetic properties. Figure 8 shows micrographs of the alloy aged at 640°C for 20 min, 1 h, and 3 h in a magnetic field of 2 kOe and their corresponding laser optical diffraction patterns. The bright field micrograph, Fig. 8(A), shows that the α_1 phase is oriented almost randomly. However, the corresponding laser optical diffraction, Fig. 8(a),

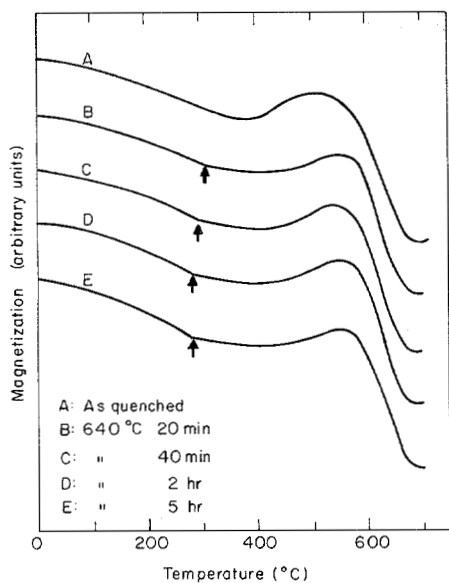


Fig. 6. Magnetization as function of temperature of alloy aged at 640°C.

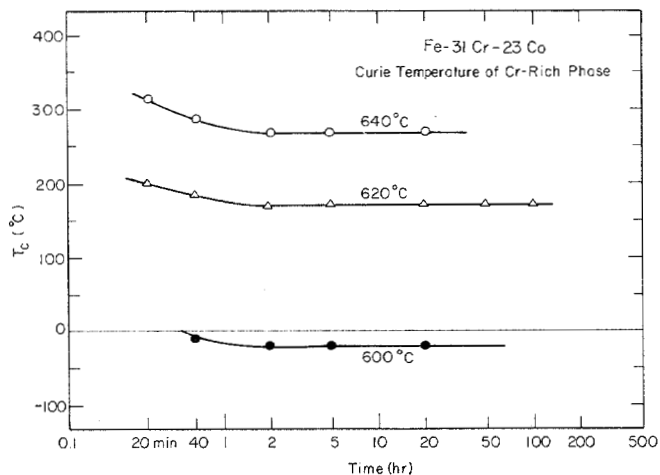


Fig. 7. Curie temperatures of Cr-rich phase aged at various temperatures as function of aging time.

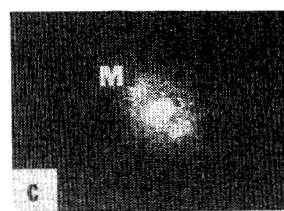
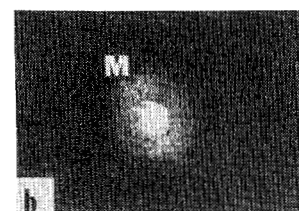
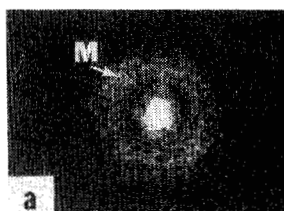
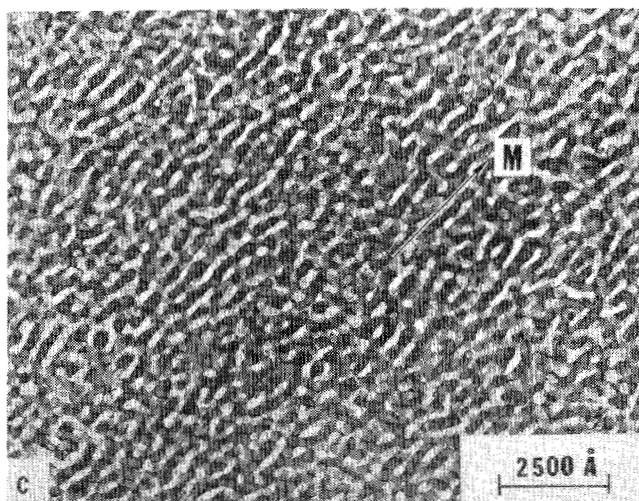
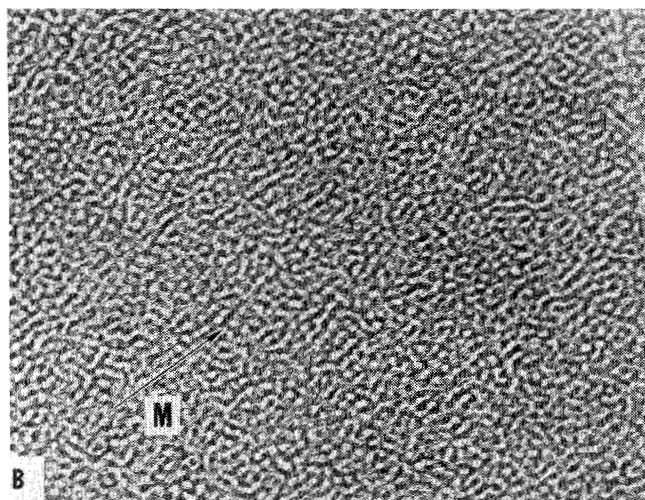
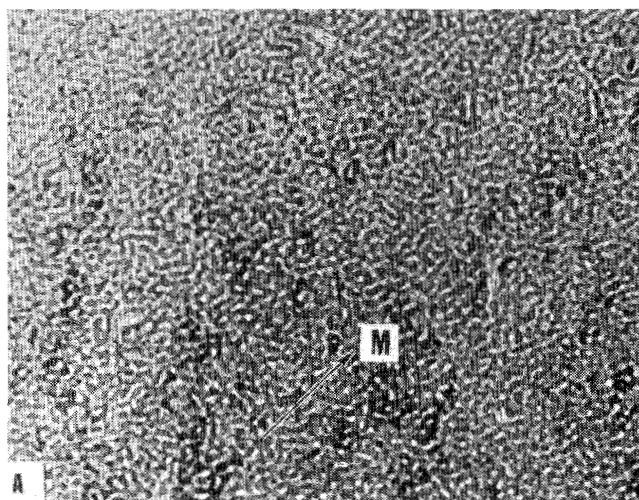


Fig. 8. Bright field micrographs of alloy aged at 640°C in magnetic field of 2 kOe for (A) 20 min, (B) 1 h, (C) 3 h, and their corresponding laser optical diffraction patterns (a), (b), and (c).

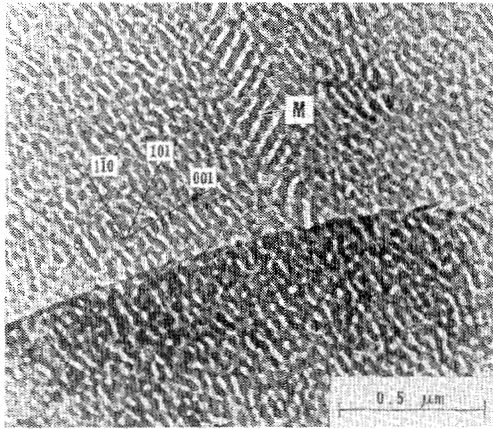


Fig. 9. Bright field micrograph taken from alloy magnetically aged at 640°C for 3 h with localized deviation in particle alignment shown at M .

exhibits peaked intensities (marked M), which implies some tendency for the α_1 phase to be aligned along this direction. The remanence in this state is nearly $0.6 I_s$ (I_s is the saturation magnetization).

Prolonged thermomagnetic aging causes the α_1 phase to be more elongated parallel to the direction marked M , as shown in Fig. 8(B), (C) and the corresponding laser optical diffraction patterns Fig. 8(b), (c). The remanence after magnetic aging for 1 h increases to almost $0.9 I_s$. This remanence remains unchanged after step aging. The high remanence indicates that the ferromagnetic α_1 phase is elongated along the direction of the applied magnetic field, independent of crystal orientation [3]. This stems from the fact that the decomposition process is found to be isotropic during the early stage of aging for at least 1 hr. The independence of the magnetic properties from the crystal orientation is already confirmed by the measurements of magnetic properties of single crystals of the alloy [9].

When the thermomagnetic aging time exceeds 2 h, the remanence decreases to about $0.8 I_s$. This decrease can possibly be explained as follows. Under ideal circumstances, even after prolonged aging in a magnetic field, the α_1 phase would maintain its alignment parallel with the applied field. However, the present observation suggests that, in fact, the α_1 phase cannot maintain this alignment in certain localized areas such as that marked M in Fig. 9. It is believed that in these areas particle alignment is highly affected by the elastic constraints of the matrix, since elastic strain energy minimization favors a $\langle 100 \rangle$ particle growth direction. Therefore, the exact direction of alignment within these regions is determined by a balance between the applied magnetic field and elastic strain field of the matrix. Therefore, the optimum time for the thermomagnetic treatment is limited from 40 min to 1 hr at 640°C . The field strength for the thermomagnetic treatment should be over 2 kOe [10].

C. Step Aging

It is reported that step aging has a beneficial effect not only on improving the magnetic properties of Fe-Cr-Co alloys [1] but also on improving the mechanical properties of Cu-Ni-Fe alloys [11]. Figure 10(a) shows the microstructure taken

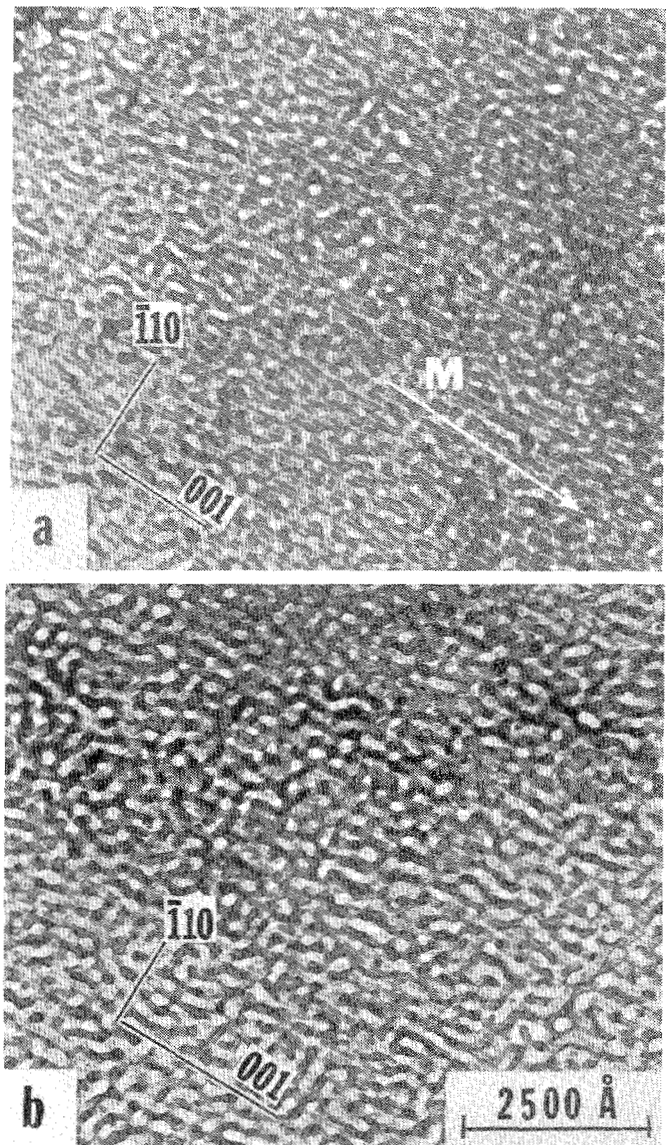


Fig. 10. (a) Micrograph of alloy aged at 640°C for 40 min in magnetic field of 2 kOe, $H_c \sim 130$ Oe. (b) Micrograph of alloy step aged at 620°C for 20 min and 600°C for 1 h after thermomagnetic treatment, $H_c \sim 410$ Oe.

from the alloy aged at 640°C for 40 min in a magnetic field of 2 kOe. The ferromagnetic phase is somewhat elongated along the direction of the magnetic field and has an interpenetrating rod-like morphology. The rod diameter is about 100 \AA and the rod length 280 \AA , giving a ratio of length to diameter of nearly 3.

Figure 10(b) shows the microstructure of the alloy given a thermomagnetic treatment at 640°C for 40 min and subsequently step aged at 620°C for 20 min and at 600°C for 1 hr. Throughout step aging it is found that the ratio of length to diameter of the α_1 phase remains essentially unchanged (130 \AA in diameter, 370 \AA in length) and that the volume fraction of the α_1 phase increases slightly from 45% to 55%. The main change during step aging is that of composition of the two phases, which is confirmed by the measurement of the Curie temperature of the α_2 phase of the step aged alloy [2]. The α_2 phase is magnetic at room temperature just after the

thermomagnetic treatment, but it becomes nonmagnetic after step aging. Therefore, the increase in coercivity during step aging is believed to be associated with a change in composition of the two phases, resulting in an increase in the difference between the magnetization intensities of the two phases.

DISCUSSION

The present microstructural observations are consistent with the results of the reported miscibility gap in the Fe-Cr-Co system [2].

The decomposition process of the alloy in the early stages of aging appears to be isotropic. The direct evidence for this is the halo-type diffuse satellites in the corresponding electron diffraction pattern (Fig. 3(a), (b)) which can be reproduced by laser optical diffraction (Fig. 8(a)). The isotropic nature of the decomposition of the Fe-Cr-Co alloy is very much different from the decomposition observed in Alnico alloys, which tend to decompose along the $\langle 100 \rangle$ directions [12], [13]. Thus the effect of thermomagnetic treatments on the microstructures of these alloys must also be different. The ferromagnetic phase in Alnico alloys preferentially grows along the $\langle 100 \rangle$ axis of each grain that is closest to the magnetic field direction [12]. However, the α_1 phase in Fe-Cr-Co alloys is elongated along the direction of the applied magnetic field, independent of the crystal orientation of the grains [3].

The properties of Alnico alloys can be further improved with an alloy which has a $\langle 100 \rangle$ texture [13], utilizing the anisotropic decomposition to more efficiently elongate the ferromagnetic phase in the direction of the applied magnetic field. The Fe-Cr-Co alloys are not improved by such treatments [9].

One possible method to improve the magnetic properties of Fe-Cr-Co alloys should be that of adding these elements which make the decomposition anisotropic, as Ti additions do in Alnico 9 [13]. This means increasing the elastic strain energy during decomposition. An example of such an element in this system is reported to be Mo [1], [14]. Although the addition of Mo to Fe-Cr-Co improves the magnetic properties [1], it is not a practically attractive method since Mo stimulates the formation of the embrittling σ phase. In order to further improve the magnetic properties while retaining good workability of the alloy, investigations of other quaternary alloying additions are clearly required. It is shown that isothermal aging itself fails to produce the optimum microstructure for good Fe-Cr-Co magnets. Aging at 640°C does not develop the nonmagnetic α_2 phase. Aging at 600°C also produces an undesirable microstructure because it results in the dispersion of the nonmagnetic α_2 phase within the α_1 phase. However, it is shown here that these problems can be overcome by step aging, which gives a microstructure of the elongated ferromagnetic α_1 phase imbedded in the paramagnetic α_2 phase.

It should be emphasized that this step aging method to produce the desired microstructure is valid only when the step aging temperature interval ($\Delta T = T_{\text{step } n} - T_{\text{step } n-1}$) is small. When the alloy is aged at low temperatures (580°C or 560°C) after thermomagnetic treatment ($\Delta T \geq 60^\circ\text{C}$), secondary decomposition takes place as shown in Fig. 11. This secondary decomposition results in a deterioration of the magnetic

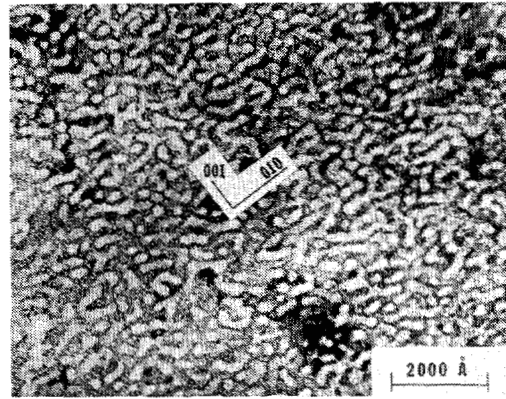


Fig. 11. Micrograph of alloy aged at 560°C for 4 h after thermomagnetic treatment at 640°C for 1 h, $H_c \sim 160$ Oe, showing the secondary decomposition.

properties of the alloy. A possible explanation of this may be that as the diameter of the decomposed phase is around 45 \AA , this phase could behave as a superparamagnetic domain [15].

CONCLUSION

The microstructures of an Fe-31wt%Cr-23wt%Co permanent magnet alloy after isothermal aging, thermomagnetic treatment, and step aging have been studied in connection with their magnetic properties. The morphology of the microstructure is very sensitive to the aging temperature. The volume fraction of the two phases varies with aging temperature. The decomposition process appears to be isotropic, being associated with halo-type diffuse satellites in the diffraction pattern. Continued aging develops a periodically modulated structure along $\langle 100 \rangle$. The lattice imaging technique reveals that the two phases are coherent. Curie temperature measurements show that decomposed phases reach their equilibrium composition after about two hours aging. Isothermal aging itself produces undesirable microstructures. Aging at 640°C develops the magnetic Cr-rich phase. Aging at 600°C produces a nonmagnetic Cr-rich phase dispersed within the Fe-rich phase. The optimum thermomagnetic treatment of the alloy involves aging at 640°C for 40 min to 1 h in a magnetic field of 2 kOe. The ferromagnetic phase is then elongated along the direction of the applied magnetic field, independent of crystal orientation. Step aging produces a beneficial microstructure, viz., the elongated ferromagnetic α_1 phase imbedded in the paramagnetic α_2 phase. The increase in coercivity by step aging is found to be associated with a change in composition of the two decomposed phases, the morphology of the iron-rich phase remaining unchanged.

REFERENCES

- [1] H. Kaneko, M. Homma, and K. Nakamura, "New Ductile Permanent Magnet of Fe-Cr-Co System," *AIP Conf. Proc.*, no. 5, p. 1088 (1971).
- [2] H. Kaneko, M. Homma, K. Nakamura, M. Okada, and G. Thomas, "Phase Diagram of Fe-Cr-Co Permanent Magnet System," *IEEE Proc. on Magnetics* (September 1977).
- [3] M. Okada, M. Homma, H. Kaneko, and G. Thomas, "The Microstructure of Fe-Cr-Co-Nb-Al Permanent Magnet," *34th Ann. Proc. EMSA*, p. 606 (1976).
- [4] G. Thomas, "High Voltage and High Resolution Electron Micros-

- copy in Materials Science," *J. of Metals*, vol. 29, no. 2, p. 31 (1977).
- [5] R. Sinclair, R. Gronsky, and G. Thomas, "Optical Diffraction from Lattice Images of Alloys," *Acta Met.*, vol. 24, p. 789 (1976).
- [6] D. R. Clarke, "The Optical Reflection Transform Method," *J. of Mater. Sci.*, vol. 10, p. 172 (1975).
- [7] E. P. Butler and G. Thomas, "Structure and Properties of Spinodally Decomposed Cu-Ni-Fe Alloys," *Acta Met.*, vol. 18, p. 347 (1970).
- [8] M. Hansen, "Constitution of Binary Alloys," 2nd edition, p. 472 (McGraw-Hill, 1958).
- [9] H. Kaneko, M. Homma, M. Okada, S. Nakamura, and N. Ikuta, "Fe-Cr-Co Ductile Magnet with $(BH)_{\max} \simeq 8$ MGOe," *AIP Conf. Proc.*, no. 29, p. 620 (1975).
- [10] H. Kaneko, M. Homma, and K. Nakamura (unpublished work).
- [11] K. Kubarych, M. Okada, and G. Thomas, "Heat Treatments for Improved Mechanical Properties of CuNiFe Spinodal Alloys," *Trans. AIME* (in press).
- [12] R. D. Heidenreich and E. A. Nesbitt, "Physical Structure and Magnetic Anisotropy of Alnico 5," *J. Appl. Phys.*, vol. 23, p. 352 (1952).
- [13] K. J. De Vos, "Alnico Permanent Magnet Materials," vol. 1, *Magnetism and Metallurgy*, p. 473 (Academic Press, 1969).
- [14] R. Cremer and I. Pfeiffer, "Permanent Magnet Properties of Cr-Co-Fe Alloys," *Physica*, vol. 80B, p. 164 (1975).
- [15] C. P. Bean and J. D. Livingston, "Superparamagnetism," *J. Appl. Phys.*, vol. 30, 120S (1959).

Relationship Between Total Losses Under Tensile Stress in 3 Percent Si-Fe Single Crystals and Their Orientations Near (110) [001]

TADAO NOZAWA, TAKA AKI YAMAMOTO, YUKIO MATSUO, AND YOSHIHIRO OHYA

Abstract—The relationship between the total loss under tensile stress and the tilt angle of the [001] out of crystal surface β was studied in 3 percent Si-Fe single crystals.

The total loss largely depends upon β . When β is about 2° , the total loss under tensile stress is the smallest, and the decrease of the total loss due to tensile stress is the largest. When β is less than about 2° , the total loss increases as β decreases. In the case of perfect (110) [001] orientation, the total loss is large. When β is larger than about 2° , the total loss increases as β increases.

The origins of these phenomena were studied by observing the domain structures using a high-voltage scanning-electron microscope. The 180° main domain wall spacing monotonically decreases with increasing β . When β is less than about 2° , the decrease of the 180° main domain wall spacing gives rise to the decrease of the total loss. However, when β is larger, the total loss increases in spite of a decrease of the 180° main domain wall spacing. This is attributed to the fact that the formation and annihilation of supplementary domains during ac magnetization greatly contributes to the total loss for $\beta > 2^\circ$.

INTRODUCTION

SEVERAL studies have been previously made on the relationship between domain structures and crystal orientation in 3% Si-Fe with orientation near (110) [001], [1], [2]. It

Paper received October 10, 1977. This work was presented at the Conference on Soft Magnetic Materials, Bratislava, Czechoslovakia, September 14-16, 1977.

The authors are with Process Technology R & D Laboratories, Nippon Steel Corporation, 1-1-1 Edamitsu Yawatahigashiku-Kitakyushu-shi 805, Japan.

has been found that the domain structure significantly depends on the tilt angle of the [001] out of sheet surface β , and surface closure domain density increases with increasing β , [1], [3]. The effects of tensile stress on domain structure in (110) [001] 3% Si-Fe also have been studied [4]-[7]. It has been shown that since the application of tensile stress parallel to the rolling direction removes surface closure domain, the refinement of 180° domain wall spacing occurs in order to decrease the magnetostatic energy due to surface free poles [6], [8].

It is well known that the eddy current loss in the (110) [001] crystal can be expressed in terms of the ratio of domain wall spacing to crystal thickness for a simple 180° domain structure and should be roughly proportional to the first power of the wall spacing [9]. Shilling *et al.* have studied the tensile stress dependence of domain structure and magnetic properties for both conventional and high-permeability grain-oriented 3% Si-Fe [10], [11]. It was found that the 180° wall spacing decreases greatly with increasing β by the application of tensile stress. It was suggested also that the slight tilt of the [001] out of crystal surface and tensile stress applied along the rolling direction are necessary for minimum loss due to a fine domain spacing. Dragoshanskiy *et al.* have studied in the unstressed condition the dependence of the total loss in single crystals of 3% Si-Fe on their crystallographic orientation, and have found that the loss minimum occurs at $\beta = 3^\circ$ [12]. It was concluded that not perfect, but optimum, orientation of the crystal is necessary to achieve the minimum total loss.